Construction and Building Materials 102 (2016) 478–485

Contents lists available at ScienceDirect

Construction and Building Materials

journal homepage: www.elsevier.com/locate/conbuildmat

Freeze–thaw durability of high strength concrete under deicer salt exposure

Zhichao Liu *, Will Hansen

Department of Civil and Environmental Engineering, University of Michigan, USA

HIGHLIGHTS

- Simultaneous measurement on surface scaling and moisture uptake is undertaken.
- HSC mixes are more prone to internal damage, albeit the high scaling resistance.
- A bi-linear pattern is noted for mass loss and moisture uptake of HSC mixes.
- Air-void characteristics is not a major factor in surface scaling of HSC mixes.

ARTICLE INFO

Article history:
Received 5 August 2015
Received in revised form 15 October 2015
Accepted 28 October 2015

Keywords:
High strength concrete
Durability
Freezing–thawing
Moisture uptake
Salt frost scaling
Air-void system

ABSTRACT

Freeze–thaw resistance of high strength concrete (HSC) and normal strength concrete (NSC) mixes with varying air contents was investigated by moisture uptake, mass loss and internal damage measurements. Sufficiently air-entrained HSC mixes demonstrate significant improvement in salt frost scaling resistance and the characteristics of air-void system is not a major factor. This can be attributed to the reduced capillary porosity and connectivity which curtails ice-growth promoted by capillary suction of surface liquid under freezing. A clear bi-linear pattern is found for the mass loss and moisture uptake curves of HSC mixes, the transition point of which coincides with each other. This demonstrates the importance of initial moisture condition in concrete prior to F–T test. Increased imperviousness of HSC to moisture ingress renders it more prone to long-term frost damage intrinsically, which is evidenced by much higher initial freezing strain in HSC from the length-change measurement on thin specimens at various degrees of saturation levels.

1. Introduction

Frost attack on concrete is a distress resulting from the phase transformation associated with the freezing of internal moisture. It essentially manifests itself from two aspects [1,2]: (1) generation of internal cracks and disintegration (internal pure frost attack), a common laboratory indicator of which is the decrease in relative dynamic modulus (RDM); (2) progressive removal of small pieces of paste/mortar within the surface region, which is characterized by the normalized mass loss per unit test area. The latter case is known to be more severe in magnitude under deicer salt exposure [3]. Salt frost deterioration has been recognized as one of the major concerns in concrete structures for a few decades in North America and Northern Europe where freezing temperature is prevalent and widespread use of deicing salts is common in winter [4].

High strength concrete (HSC) is characterized by a very low water–cement (w/c) ratio (typically less than 0.35) and a 28d compressive strength higher than 60 MPa [5,6]. HSC has found wide application in structures such as bridge decks, rapid repair materials to concrete pavement under potential exposure to F–T conditions. It is generally accepted that HSC has better salt scaling resistance than normal strength concrete (NSC) [7,8], which is attributed to the improved paste quality by lowering the w/c ratio [9,10]. This has been reflected in the specifications for mix proportioning of concrete under severe exposure, where a limit to w/c ratio is imposed [11,12]. However, there is a lack of full understanding for this benefit since the mechanism of salt frost deterioration is still under dispute [4,13]. A recently proposed mechanism links scaling to the exacerbated ice growth in concrete pores near the surface region promoted by the transport of external liquid made available by the presence of salt [14].

This paper makes an effort to interpret the improved salt scaling resistance of HSC by investigating the mass loss, moisture uptake

---

* Corresponding author at: Department of Civil and Environmental Engineering, 2350 Hayward, 2330 GG Brown, Ann Arbor, MI 48109-2125, USA.
E-mail address: lzc@umich.edu (Z. Liu).

http://dx.doi.org/10.1016/j.conbuildmat.2015.10.194
0950-0618/

and internal frost damage simultaneously under salt/F–T exposure in both HSC and NSC specimens. The length-change behavior of presaturated specimens was also studied to hopefully shed more light on the intrinsic frost durability of HSC.

2. Experimental

2.1. Characteristics of concrete mixtures

150 mm × 150 mm × 533 mm beams were prepared for the HSC mixes (0.33 *w*/*c* ratio) in a ready-mix plant while 150 mm by 300 mm cylinders NSC mixes (0.45 *w*/*c* ratio) were made in the laboratory. Raw materials included Type I portland cement, silica sand and limestone gravel. Commercially available superplasticizer and air-entrainer were used to achieve an 80–100 mm slump and 3.0–9.3% air content in the air-entrained concretes. In addition, 100 mm by 200 mm cylindrical specimens were prepared for non-air entrained concrete mix at each *w*/*c* ratio, from which compressive strength was tested according to ASTM C39 [15]. All the specimens were cured for one day before being demoulded and moist cured for another 27 days at 20 °C. The mix design and air void properties based on ASTM C457 [16] are listed in Table 1. The compressive strength of the two non-air entrained concrete mixes is shown in Fig. 1.

2.2. Surface scaling, internal damage, moisture absorption

Concurrent measurement of cumulative mass loss, bulk moisture uptake and internal cracking in concrete specimens under unidirectional exposure to combined salt/frost attack was undertaken using an F–T machine specified in the RILEM TC 176-IDC CIF-Test [17]. Prior to F–T exposure, the bottom surface of a pre-dried concrete specimen of 100 mm × 100 mm × 70 mm was pre-saturated in demineralized water for 7 days and the weight gain was regularly monitored. Meanwhile, additional thinner specimens (12-mm thick) from the 045–5.1% and 033–5.7% mixes were tested for moisture uptake only, such that the moisture absorption behavior could be compared with the 70 mm-thick specimen.

The pre-conditioned 70-mm thick concrete blocks were then put in contact with a 3% sodium chloride (NaCl) solution while exposed to a specific temperature profile fluctuating between 20 °C and −20 °C in 12 h for each cycle with a cooling/heating rate of 10 °C/h. The cycle starts at 20 °C and cools down to −20 °C in 4 h, followed by a 3-h isothermal stage. Then it heats up to 20 °C. During the one-hour isothermal period at 20 °C, scaled-off materials were collected and dried at 105 °C to constant weight, from which mass loss per unit surface area ML (g/m^2) was determined.

$$\text{ML (g/m}^2) = \frac{\mu_n}{A_c} \times 10^4 \tag{1}$$

where μ_n (g) is the cumulative dry weight of the scaled-off materials after the *n*th F–T cycle, A_c (cm^2) is the area of the concrete test surface.

Permanent moisture uptake in concrete is calculated from the weight measurement of the specimen and the scaled-off materials by assuming the same moisture content in the saturated scaled-off materials as in the remaining bulk concrete.

Internal damage in concrete after the *n*th F–T cycle is evaluated by the relative dynamic modulus of elasticity (RDM) calculated from the ultrasonic transit time in the coupling medium (typically water at 20 °C). The transit time is measured by a Pundit Plus ultrasonic digital indicating tester with 54 kHz transducers.

2.3. Length-change measurement by a low temperature dilatometer (LTD)

The length and temperature change of small-scale concrete prisms at varying pore saturation levels were continuously monitored by a low temperature dilatometer (LTD) during an F–T cycle. The LTD has a length-change resolution of 1.25 nm/digit and a temperature precision of 0.1 K and a liquid nitrogen dewar was equipped for low temperature control. The 10 mm × 10 mm × 90 mm specimen was cut out of the concrete cylinder or beam using a concrete saw with tapping water as the cooling medium. Prior to test, the specimen was carefully wrapped by a plastic sheet to minimize moisture loss during test. A similar F–T cycle to the salt frost scaling test was used except that an additional 3-h isothermal stage at −10 °C was added.

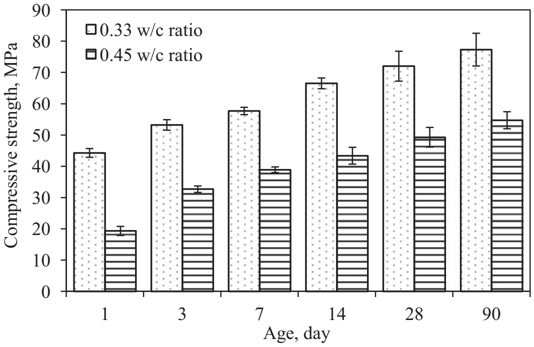

Fig. 1. Compressive strength for non-air entrained concrete mixes of two different *w*/*c* ratios.

3. Results and discussion

Internal frost damage, surface scaling and moisture uptake of HSC and NS concrete mixes are investigated on duplicate specimens. The mixes have a total air content ranging from 2.5–9.3% and a Powers' spacing factor of 62–503 μm. Most of these mixes were tested up to around 80 F–T cycles while extended period was used for the 033–5.7% mix (>150 F–T cycles).

3.1. Internal frost damage

The non-air entrained concrete specimens (033–2.5%) show severe internal cracking, as demonstrated by the rapid reduction in RDM (Fig. 2) and the generation of bulk cracks onto the top unexposed surface (Fig. 3(a)). This leads to the removal of coarse aggregate particles from the test surface (Fig. 3(b)) which exacerbates mass loss (Fig. 2). On the other hand, no internal frost damage is observed in the air-entrained mixes (Fig. 4), which is consistent with the requirement on critical spacing factor for regular frost resistance (200–250 μm) [12,18–20]. This eliminates the interference of internal bulk cracking on the surface scaling and moisture uptake results.

3.2. Surface scaling and moisture uptake properties

The moisture uptake and mass loss normalized to the area of exposed surface for the air-entrained concrete mixes are summarized in Figs. 5–9. During the 7-day presaturation stage, moisture

Table 1
Mix design and air void properties.

Mix	Mix proportion, kg/m^3			Air void results by linear traverse				
	Cement	Sand	Gravel	Air content, %		Powers' spacing factor, μm	Specific surface, mm^{-1}	Average chord length, μm
				Total	<0.5 mm			
033–2.5%	390	672	1068	2.56	0.39	503	13.72	292
033–5.7%	390	672	1068	5.70	3.53	117	33.8	118
033–6.5%	390	672	1068	6.47	3.77	111	31.9	125
033–7.8%	390	672	1068	7.78	4.56	119	26.8	149
033–8.3%	390	672	1068	8.25	6.40	71	39.0	103
033–9.3%	390	672	1068	9.32	6.19	88	24.9	161
045–5.1%	290	775	1115	5.12	4.37	104	45.3	88
045–8.1%	290	775	1115	8.08	7.16	62	53.5	75